Journal of Alloys and Compounds 481 (2009) 228–232

Contents lists available at ScienceDirect

Journal of Alloys and Compounds

journal homepage: www.elsevier.com/locate/jallcom

# Thermodynamic properties of $Pb_2PtO_4$ and $PbPt_2O_4$ and phase equilibria in the system Pb–Pt–O

K.T. Jacob[a,*], G. Rajitha[a], G.M. Kale[b]

[a] Department of Materials Engineering, Indian Institute of Science, Bangalore 560 012, India
[b] Institute for Materials Research, University of Leeds, Leeds LS2 9JT, UK

ARTICLE INFO

*Article history:*
Received 17 February 2009
Accepted 11 March 2009
Available online 24 March 2009

*Keywords:*
Thermodynamic properties
Electromotive force (emf)
Thermal analysis
Thermodynamic modeling
Oxide materials

ABSTRACT

The compounds $Pb_2PtO_4$ and $PbPt_2O_4$ were synthesized from an intimate mixture of yellow PbO and Pt metal powders by heating under pure oxygen gas at 973 K for periods up to 600 ks with intermediate grinding and recompacting. Both compounds were found to decompose on heating in pure oxygen to PbO and Pt, apparently in conflict with the requirements for equilibrium phase relations in the ternary system Pb–Pt–O. The oxygen chemical potential corresponding to the three-phase mixtures, $Pb_2PtO_4$ + PbO + Pt and $PbPt_2O_4$ + PbO + Pt were measured as a function of temperature using solid-state electrochemical cells incorporating yttria-stabilized zirconia as the solid electrolyte and pure oxygen gas at 0.1 MPa pressure as the reference electrode. The standard Gibbs free energies of formation of the ternary oxides were derived from the measurements. Analysis of the results indicated that the equilibrium involving three condensed phases $Pb_2PtO_4$ + PbO + Pt is metastable. Under equilibrium conditions, $Pb_2PtO_4$ should have decomposed to a mixture of PbO and $PbPt_2O_4$. Measurement of the oxygen potential corresponding to this equilibrium decomposition as a function of temperature indicated that decomposition temperature in pure oxygen is 1014(±2) K. This was further confirmed by direct determination of phase relations in the ternary Pb–Pt–O by equilibrating several compositions at 1023 K for periods up to 850 ks and phase identification of quenched samples using X-ray diffraction (XRD), scanning electron microscopy (SEM) and energy dispersive X-ray spectroscopy (EDS). Only one ternary oxide $PbPt_2O_4$ was stable at 1023 K under equilibrium conditions. Alloys and intermetallic compounds along the Pb–Pt binary were in equilibrium with PbO.



## 1. Introduction

As part of studies on the thermodynamics of interaction between lead containing ferroelectric oxides and Pt electrodes, phase relations in the system Pb–Pt–O were explored and thermodynamic properties of the two ternary oxides present at ambient pressure were determined. Anderson et al. [1] have reported $PbPt_2O_4$ formation at the interface between lead–zirconate–titanate (PZT) solid solution and Pt during PZT deposition using high-throughput modified molecular-beam epitaxy (MBE) technique. There are three known ternary oxides in the Pb–Pt–O system; $Pb_2Pt_2O_{6.5}$, $Pb_2PtO_4$ and $PbPt_2O_4$. The cubic pyrochlore $Pb_2Pt_2O_{6.5}$ with lattice parameter $a = 1.0291$ nm has been synthesized at 973 K and pressure $P/P^\circ = 3000$, where $P^\circ$ represents standard pressure [2]. The other two compounds are stable at ambient pressure. The compound $Pb_2PtO_4$ has orthorhombic crystal structure (space group *Pbam*, $Z = 2$) with lattice parameters $a = 0.9115$, $b = 0.7941$ and $c = 0.6306$ nm [3]. The compound is an insulator with $Pt^{4+}$ ions in octahedral environment. $PtO_6$ octahedra are edge shared along the *c*-axis direction to form rutile-type chains. The $Pb^{2+}$ ions are stacked in rows in the channels between the chains. The compound $PbPt_2O_4$ is a metallic conductor and has triclinic crystal structure (space group $P\bar{1}$, $Z = 2$) with lattice parameters $a = 0.61173$, $b = 0.66489$ and $c = 0.55523$ nm, $\alpha = 97.195^\circ$, $\beta = 108.827^\circ$, $\gamma = 115.213^\circ$ [4]. Pt is in two oxidation states; $Pt^{2+}$ is in square planar and $Pt^{4+}$ in octahedral environment. $PtO_4$ groups are columnar stacked along the *c*-axis. These stacks are held by other planar $PtO_4$ groups to constitute $Pt_3O_8$ sheets. The sheets are linked together by $PtO_6$ octahedra to form a three-dimensional network. The Pb atoms are surrounded by six oxygen forming distorted octahedra. The metallic conductivity is consistent with the short Pt–Pt bonds in the columnar stacks of $PtO_4$ groups along the *c*-direction [5]. In the literature, there is neither thermodynamic data for the two ternary oxides nor information of phase relations in the ternary system Pb–Pt–O.

Earlier studies on Pb-containing systems of interest in the processing of piezoelectric ceramics were concerned with thermodynamic properties of lead zirconate [6], lead titanate [7], lead aluminates [8], lead ruthinate [9] and $Pb(Zr,Ti)O_3$ (PZT) solid solution [10]. Phase equilibria in the systems Pb–Ru–O [9],

* Corresponding author.
*E-mail addresses:* katob@materials.iisc.ernet.in, ktjacob@hotmail.com (K.T. Jacob).

0925-8388/$ – see front matter © 2009 Elsevier B.V. All rights reserved.
doi:10.1016/j.jallcom.2009.03.051

$PbO–RuO_2–TiO_2$ [11] and $RuO_2–TiO_2$ in air [12] have been delineated. Also available is a thermodynamic analysis of the interaction between $Pb(Zr,Ti)O_3$ solid solutions and $RuO_2$ electrodes as a function of PZT composition, temperature and oxygen partial pressure [13].

## 2. Experimental aspects

### 2.1. Materials

The compounds $Pb_2PtO_4$ and $PbPt_2O_4$ were synthesized from yellow lead monoxide (PbO), platinum metal and pure oxygen gas at high temperature. PbO and Pt powders, each of purity greater than 99.9%, were thoroughly mixed in the appropriate stoichiometric ratios in an agate mortar, mixture compacted at 100 MPa pressure in a steel die, and the pellet heated under flowing oxygen gas at 973 K until completion of reaction. At intervals of ~90 ks the pellets were quenched in liquid nitrogen, reground and recompacted for further heat treatment. After each quench, powders were examined at room temperature by X-ray diffraction (XRD) to assess the progress of reaction. The formation of dark brown $Pb_2PtO_4$ was complete in ~300 ks, whereas ~540 ks was required for dark grey $PbPt_2O_4$. The Pb and Pt content of the compounds were determined by chemical analysis and the oxygen content by mass loss measurement during hydrogen reduction at 823 K. The compounds were found to be essentially stoichiometric. The XRD patterns of the two compounds recorded in this study were almost identical to those reported in the literature [3–5]. The lattice parameters for $PbPt_2O_4$ obtained in this study ($a = 0.61168$, $b = 0.66495$ and $c = 0.55510$ nm, $\alpha = 97.196^\circ$, $\beta = 108.819^\circ$, $\gamma = 115.225^\circ$) showed very minor difference from the values given by Obbade et al. [4].

The intermetallic compounds $PbPt_3$ and PbPt, required for phase equilibrium studies on the system Pb–Pt–O, were prepared by melting a mixture of metals in the required ratios at 1673 and 1273 K, respectively. The compound $PbPt_3$ was annealed at 1073 K and PbPt at 1023 K for ~20 ks. XRD confirmed formation of the compounds.

### 2.2. Decomposition studies

Thermal stability of $Pb_2PtO_4$ and $PbPt_2O_4$ was investigated using differential thermal analysis (DTA) and thermo-gravimetric analysis (TGA) in pure oxygen gas both on heating and cooling. Examined by XRD and EDS were the residue obtained after DTA/TGA experiments. In a few experiments, after recording the decomposition at high temperature, the samples were rapidly cooled under flowing argon gas and the residue examined by XRD and EDS.

### 2.3. Electrochemical measurements

The emf of the following cells were measured as a function of temperature from 875 K at intervals of 25 K until the emf became marginally negative, which indicated that the oxygen pressure over the working electrode was above atmospheric:

$$Pt, PbPt_2O_4 + PbO + Pt/(Y_2O_3)ZrO_2/RuO_2, O_2(0.1\ MPa), Pt \quad (1)$$

$$Pt, Pb_2PtO_4 + PbO + Pt/(Y_2O_3)ZrO_2/RuO_2, O_2(0.1\ MPa), Pt \quad (2)$$

$$Au, Pb_2PtO_4 + PbPt_2O_4 + PbO/(Y_2O_3)ZrO_2/RuO_2, O_2(0.1\ MPa), Au \quad (3)$$

The cells are written such that the right-hand side electrodes are generally positive. In each cell the oxygen pressure at the reference electrode on the right-hand side was higher than that over the working electrode consisting of three condensed phases, except at the highest temperature when the dissociation pressure marginally exceeded that of the reference gas. The upper temperature limit was signalled by marginally negative value of the emf.

Initially measurements were made on cells (1) and (2). As discussed later, an analysis of the electrochemical measurements indicated that the working electrode of cell (2) was in metastable equilibrium. Hence, cell (3) was designed based on stable equilibrium phase mixture at the working electrode. Gold was used as an inert electrical leads, since use of Pt could change phase relations at least at the points of contact between the electrical lead and the measuring electrode.

The apparatus used for electrochemical measurements was similar to that described earlier [14] with minor variations. Shown in Fig. 1 is a schematic diagram of the cell assembly. Since the oxygen partial pressures over the electrodes of the cell were expected to be high, a closed system was used for measurements. The three-phase electrode was placed in a stabilized zirconia crucible, which was sealed in an evacuated quartz tube. The equilibrium oxygen partial pressure was established by the decomposition of the ternary oxide present at the electrodes at high temperature. Used as the reference electrode was pure oxygen gas at standard pressure. Yttria-stabilized zirconia (YSZ) tube, containing 12 mol% $Y_2O_3$, closed at one end, was used as the solid electrolyte. YSZ is an oxygen ion conductor with ionic transport number greater than 0.999 at the temperatures and oxygen partial pressures encountered at the electrodes of the cells used in this study. The tube was vacuum tested for leaks and found to be impervious.

The oxygen reference electrode is generally fabricated by platinizing the surface to the YSZ tube, spheroidizing the thin deposit by heat treatment, and pressing a Pt gauze with an attached Pt lead against it. Passed over the platinized surface is a stream of oxygen gas. The finely dispersed Pt catalyzes the conversion of oxygen molecules in the gas to oxygen ions in the solid electrolyte at the triple phase boundary. Such electrodes work well above 873 K. Better catalysts are required for lower temperatures. Periaswami et al. [15] have shown that $RuO_2$ dispersed on the YSZ surface can lower the response temperature to 773 K. In this study, an attempt was made to enhance the temperature range of measurement by using spheroidized $RuO_2$ dispersion. A few drops of 10% aqueous solution of $RuCl_3$ was introduced over the inner flat surface of the YSZ tube. The tube was heated to 1073 K for 300 s under flowing air. Obtained by this treatment was a highly adherent dispersed $RuO_2$ black deposit. Pressed against this surface by an alumina tube was a Pt mesh with an attached Pt lead.

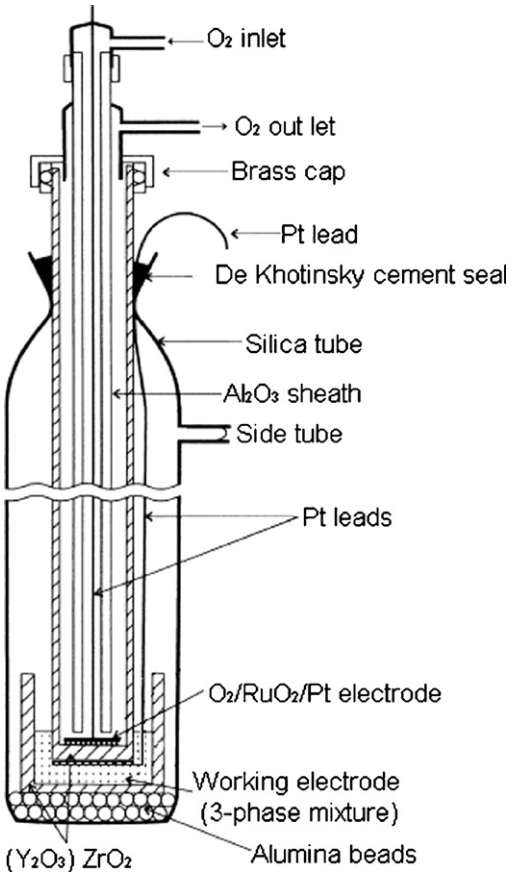


**Fig. 1.** Schematic diagram of the cell assembly.

The three-phase mixtures were compacted in YSZ crucibles to form the working electrodes of the three cells. The components of the mixture were taken in the molar ratio 1:1:1.5, with an excess of the phase that decomposed at high temperature to establish the oxygen pressure over the electrode. The solid electrolyte tube was pressed against the mixture, with a Pt mesh sandwiched in between. The assembly was enclosed in an outer quartz tube. At the cold end, the gap between the neck of the quartz tube and the YSZ tube was sealed with De Khotinsky cement as shown in the diagram. After assembling the cell the quartz tube was evacuated through a side arm to a pressure of 0.1 Pa and then flame-sealed. The entire assembly shown in Fig. 1 was placed inside a vertical resistance furnace, with the electrodes located in the even-temperature zone (±1 K). The cement seal located at the top of the assembly was maintained at room temperature throughout the measurements. A Faraday cage made of stainless steel foil was placed between the furnace tube and the cell assembly. The foil was earthed to minimize induced emf on cell leads. The temperature of the cell was measured with a Pt/Pt–13%Rh thermocouple, checked against the melting point of gold. A high-impedance digital voltmeter with a sensitivity of 0.01 mV measured the cell potentials.

### 2.4. Isothermal section at 1023 K of Pb–Pt–O phase diagram

The isothermal section was explored by equilibrating compacted mixtures of metals/intermetallics and oxides at 1023 K for prolonged periods up to 850 ks and phase identification after quenching in liquid nitrogen or chilled mercury. The phase composition of the samples was unaltered by further heating. During the total equilibration period, the samples were quenched twice, ground to −325 mesh, and recompacted using a steel die for further heat treatment. Chosen for study were 11 samples representing nine compositions inside the ternary triangle. In

two cases, samples of the same average composition were prepared using different starting materials. The samples containing metallic phases were contained in YSZ crucibles and sealed in evacuated quartz tubes for equilibration. Oxide mixtures were equilibrated under pure oxygen gas. Optical microscopy (OM), scanning electron microscopy (SEM), energy dispersive spectroscopy (EDS) and powder X-ray diffraction (XRD) at room temperature identified the equilibrium phases present in the quenched samples.

## 3. Results and discussion

### 3.1. Decomposition of $Pb_2PtO_4$ and $PbPt_2O_4$

DTA of $Pb_2PtO_4$ in pure oxygen gas showed an endothermic peak corresponding to decomposition, starting at 1086 K and ending at 1131 K, with maximum height at 1112 K. The decomposition was not reversible since no peak was observed during cooling. The examination of the residue by XRD after cooling in oxygen indicated the presence of yellow PbO with orthorhombic structure and Pt metal. The same phases were identified when the decomposition products were cooled under argon gas. TGA in oxygen confirmed the onset of decomposition at 1085 K; the total mass loss during decomposition corresponded to the loss of one molecule of diatomic oxygen gas from $Pb_2PtO_4$.

DTA of $PbPt_2O_4$ in pure oxygen gas exhibited an endothermic decomposition peak, starting at 1111 K and ending at 1160 K, with peak maximum at 1141 K. No peak was observed during cooling. The examination of the residue after cooling in oxygen and argon indicated the presence of yellow PbO and Pt. TGA in oxygen confirmed the onset of decomposition at 1110 K; the mass loss during decomposition corresponded to the escape of one and a half molecules of oxygen gas from the compound.

### 3.2. Electrochemical measurements

The emf of cell (1) was measured in the temperature range from 875 to 1125 K, cell (2) from 875 to 1100 K, and cell (3) from 875 to 1025 K. After a change in temperature, the emf of cells (1) and (2) became steady in 3–10 ks after the attainment of thermal equilibrium; longer periods were required at the lower temperatures. The response of cell (3) was very sluggish, requiring up to 80 ks to register steady values. Constancy of emf was checked over 120 ks.

The reversibility of the cells was checked by microcoulometric titration in both directions. The emfs were found to gradually return to the same value after essentially infinitesimal displacement of the equilibrium oxygen potential of the working electrode to higher and lower values for cells (1) and (2). The response of cell (3) after titration was too sluggish for the method to be effectively used, except at the higher temperatures. The reversibility of the cells was also tested by temperature cycling. The same emf was registered when approached from lower and higher temperatures.

The reversible emf of the three cells is plotted versus temperature in Fig. 2. The emfs of all the cells decrease linearly with increasing temperature. The least-squares regression analysis gives the following expressions for the temperature-dependence of emf:

$$E_1(\pm 0.66)/\mathrm{mV} = 478.40 - 0.43175T \quad (4)$$

$$E_2(\pm 0.54)/\mathrm{mV} = 477.26 - 0.4408T \quad (5)$$

$$E_3(\pm 0.64)/\mathrm{mV} = 461.72 - 0.4549T \quad (6)$$

The quoted uncertainty limits correspond to twice the standard error estimate ($2\sigma$). Since the ionic transport number of YSZ solid electrolyte is greater than 0.999 under the experimental conditions used in this study, the emfs are related to the difference in oxygen chemical potentials at the two electrodes by the Nernst equation. Further, as pure oxygen at 0.1 MPa pressure was used as the reference electrode, the emf directly gives the chemical potential of oxygen at the working electrode.

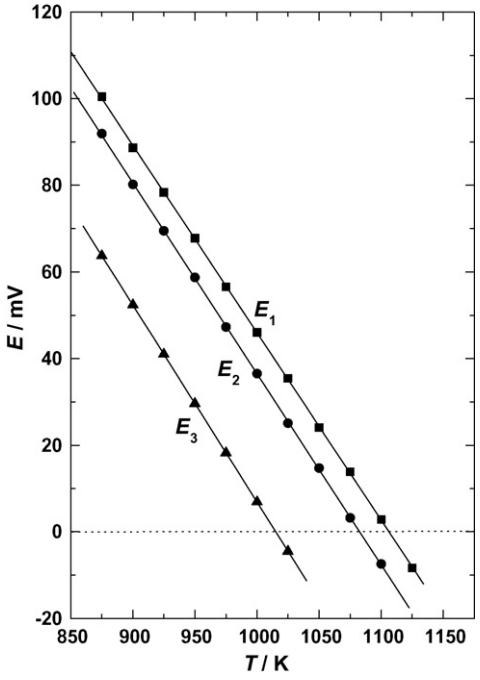


**Fig. 2.** Variation of the emf of cells (1)–(3) with temperature.

The oxygen potential ($\Delta\mu_{O_2} = RT \ln P_{O_2}$) at the working electrode of cell (1) defined by the reaction,

$$\mathrm{PbO(ortho)} + 2\mathrm{Pt} + 1.5\mathrm{O_2} \rightarrow \mathrm{PbPt_2O_4} \quad (7)$$

can be computed from the emf since there is negligible mutual solubility between the solid phases. The standard Gibbs energy of formation of $PbPt_2O_4$ from yellow PbO with orthorhombic structure, Pt metal and oxygen gas according to reaction (7) is related to the oxygen potential:

$$\Delta G_7^\circ(\pm 385)/\mathrm{J\,mol^{-1}} = 1.5\Delta\mu'_{O_2} = -6FE_1 = -276{,}951 + 249.94T \quad (8)$$

The "second-law" enthalpy of formation of $PbPt_2O_4$ from PbO, Pt and $O_2$ according to reaction (7) at a mean temperature of 1000 K is −276.95 (±1.45) kJ/mol. The corresponding entropy change is −249.94 (±1.42) J/mol K. The decomposition temperature of $PbPt_2O_4$ computed using Eq. (8) in pure oxygen at standard pressure is 1108(±2) K, and in air 1028(±2) K. The decomposition in pure oxygen derived from emf measurements is in good agreement with the values of 1111 and 1110 K derived from DTA and TGA results obtained during heating. Dynamic techniques, where temperature is continuously varied, tend to register decomposition at temperatures slightly higher than that obtained from a series of essentially equilibrium measurements at constant temperatures. It is to be noted that the onset temperature, rather that peak maximum temperature, for decomposition in DTA and DTGA studies correlates better with thermodynamic measurements. The decomposition temperature of $PbPt_2O_4$ in air (1028 K) obtained from electrochemical measurements compares with values of 1057 K [4] and 1023 K [5] reported in the literature using DTA.

The oxygen potential at the working electrode of cell (2) and the standard Gibbs energy change for the reaction,

$$2\mathrm{PbO(ortho)} + \mathrm{Pt} + \mathrm{O_2} \rightarrow \mathrm{Pb_2PtO_4} \quad (9)$$

computed from the emf are given by,

$$\Delta G_9^\circ(\pm 210)/\mathrm{J\,mol^{-1}} = \Delta\mu''_{O_2} = -4FE_2 = -184{,}194 + 170.12T \quad (10)$$

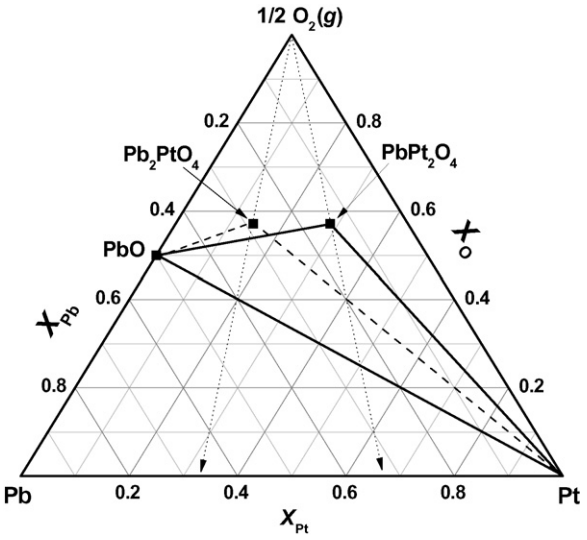


**Fig. 3.** Overlapping three-phase fields generated by the decomposition of $Pb_2PtO_4$ and $PbPt_2O_4$ in pure oxygen.

The first (temperature-independent) term on the right-hand side of Eq. (10) gives the enthalpy of formation of $Pb_2PtO_4$ from PbO, Pt and $O_2$ according to reaction (9) [−184.19(±0.93) kJ/mol] at a mean temperature of 988 K. The second (temperature-dependent) term with a change in sign gives the corresponding entropy of formation [−170.12 (±0.93) J/mol K]. The decomposition temperature of $Pb_2PtO_4$ corresponding to reaction (9) in pure oxygen at 0.1 MPa pressure is 1083(±2) K and in air 1006(±2) K. This result from thermodynamic measurements is in good accord with direct decomposition studies using DTA/TGA, which indicate the onset of decomposition at 1086 K in pure oxygen. Bettahar et al. [3] reported a value of 1008 K in air using DTA.

Three-phase equilibria defining the oxygen potentials at the working electrodes of cells (1) and (2) are displayed on a Gibbs triangle in Fig. 3. It is seen that the two three-phase regions overlap in violation of the topographical rules of construction of ternary phase diagrams. This suggests that one of the three-phase fields may correspond to metastable equilibrium. To identify the metastable equilibrium, the standard Gibbs energy change for the reaction,

$$3Pb_2PtO_4 + Pt \rightarrow 4PbO + 2PbPt_2O_4 \quad (11)$$

was computed from the results obtained in this study (Eqs. (8) and (10)):

$$\Delta G^{\circ}_{11}(\pm 740)/\mathrm{J\,mol^{-1}} = -1320 - 10.48T \quad (12)$$

The result indicates that under equilibrium conditions a mixture of $Pb_2PtO_4$ + Pt must react to give a mixture of PbO + $PbPt_2O_4$. Thus, the equilibrium between three condensed phases represented by reaction (9) is metastable. The formation of $PbPt_2O_4$ from $Pb_2PtO_4$ appears to very sluggish and does not occur in the time frame of DTA/TGA measurements in oxygen. Heating $Pb_2PtO_4$ beyond its equilibrium decomposition temperature results in its decomposition to PbO and Pt. Electrochemical proof for this hypothesis comes from measurements on cell (3). The oxygen potential at the working electrode of this cell defined by the reaction,

$$3PbO(\mathrm{ortho}) + PbPt_2O_4 + 0.5O_2 \rightarrow 2Pb_2PtO_4 \quad (13)$$

$$\Delta G^{\circ}_{13}(\pm 125)/\mathrm{J\,mol^{-1}} = 0.5\Delta\mu'''_{O_2} = -2FE_3 = -89{,}098 + 87.78T \quad (14)$$

is almost identical to that calculated from the results from cells (1) and (2) [$\Delta G^{\circ}_{13}/\mathrm{J\,mol^{-1}} = -91,437 + 90.3T$], although the separate enthalpy and entropy terms show some difference. The decomposition of $Pb_2PtO_4$ under true equilibrium conditions defined by reaction (13) occurs at 1014(±2) K in pure oxygen and at 945(±2) K in air. Since the emf of cell (3) was measured over a smaller range of temperature, greater reliance is placed on measurements on cell (2) for deriving thermodynamic properties of $Pb_2PtO_4$. The results obtained in this study clearly demonstrate that metastable equilibria are as valuable as stable equilibria in determining thermodynamic properties of complex oxides. Direct phase equilibrium studies provide further evidence of correct phase relations is the system Pb–Pt–O.

Thermodynamic properties of $PbPt_2O_4$ and $Pb_2PtO_4$can be evaluated at 298.15 K from the results of this study, using average values of 18.84, 12.56 and 6.28 J/mol K for change in heat capacity ($\Delta C^{\circ}_p$) for reactions (7), (9) and (13), respectively [16]. The standard enthalpy and entropy of formation of $PbPt_2O_4$ according to reaction (7) at 298.15 K are −290.2(±3.3) kJ/mol and −272.74 (±3) J/mol K, respectively. For $Pb_2PtO_4$ the standard enthalpy and entropy of formation according to reaction (9) at 298.15 K are −193.0(±2.7) kJ/mol and −185.17(±2.5) J/mol K. The standard enthalpies of formation from elements at 298.15 K are $\Delta H^{\circ}_{298.15}(\pm 3.6)/\mathrm{kJ\,mol^{-1}} = -508.2$ for $PbPt_2O_4$, and $\Delta H^{\circ}_{298.15}(\pm 3)/\mathrm{kJ\,mol^{-1}} = -829.1$ for $Pb_2PtO_4$. The corresponding standard entropies are $S^{\circ}_{298.15}(\pm 3.4)/\mathrm{J\,mol^{-1}\,K^{-1}} = 186.93$ for $PbPt_2O_4$ and $S^{\circ}_{298.15}(\pm 2.8)/\mathrm{J\,mol^{-1}\,K^{-1}} = 199.1$ for $Pb_2PtO_4$. The auxiliary thermodynamic data used in the calculation are $\Delta H^{\circ}_{298.15}(\pm 0.63)/\mathrm{kJ\,mol^{-1}} = -218.06$ and $S^{o}_{298.15}(\pm 0.21)/J \cdot \mathrm{mol^{-1}} \cdot K^{-1} = 68.7$ for PbO [17], $S^{\circ}_{298.15}(\pm 0.4)/\mathrm{J\,mol^{-1}\,K^{-1}} = 41.63$ for Pt [18], and $S^{\circ}_{298.15}(\pm 0.04)/\mathrm{J\,mol^{-1}\,K^{-1}} = 205.15$ for $O_2$ gas [17]. It would be useful to confirm the derived values for enthalpy of formation and entropy of the two ternary oxides by more direct calorimetric techniques.

**Table 1**
Experimental details of phase equilibrium studies at 1023 K.

| Expt. no. | Materials used for sample preparation | Average composition of sample | | | Duration of equilibration (ks) | Phases identified after equilibration | Techniques used |
|---|---|---|---|---|---|---|---|
| | | $X_{Pt}$ | $X_{Pb}$ | $X_O$ | | | |
| 1 | $Pb_2PtO_4$ | 0.1447 | 0.2842 | 0.571 | 850 (in $O_2$) | PbO + $PbPt_2O_4$ | XRD, EDS |
| 2 | Pt + $Pb_2PtO_4$ | 0.184 | 0.272 | 0.544 | 824 | PbO + $PbPt_2O_4$ | XRD |
| 3 | Pb + $PbPt_2O_4$ | 0.2 | 0.4 | 0.4 | 768 | PbO + Pt | XRD, EDS |
| 4 | Pt + $Pb_2PtO_4$ | 0.4 | 0.2 | 0.4 | 674 | PbO + $PbPt_2O_4$ + Pt | XRD |
| 5 | Pt + PbPt + $PbPt_2O_4$ | 0.4 | 0.2 | 0.4 | 739 | PbO + $PbPt_2O_4$ + Pt | XRD |
| 6 | Pt + $PbPt_2O_4$ | 0.5 | 0.1 | 0.4 | 785 | $PbPt_2O_4$ + Pt | XRD |
| 7 | Pb + $PbPt_3$ + PbO | 0.25 | 0.55 | 0.2 | 797 | PbO + PbPt + $Pb_{0.69}Pt_{0.31}(l)$ | XRD, EDS |
| 8 | Pb + $PbPt_3$ + PbO | 0.374 | 0.426 | 0.2 | 821 | PbO + PbPt + $PbPt_3$ | XRD, EDS |
| 9 | PbPt + $Pb_2PtO_4$ | 0.374 | 0.426 | 0.2 | 835 | PbO + PbPt + $PbPt_3$ | XRD |
| 10 | PbPt + Pt + $PbPt_2O_4$ | 0.5 | 0.3 | 0.2 | 835 | PbO + $PbPt_3$ + Pt | XRD, EDS |
| 11 | Pt + $Pb_2PtO_4$ | 0.7 | 0.1 | 0.2 | 772 | PbO + $PbPt_2O_4$ + Pt | XRD |

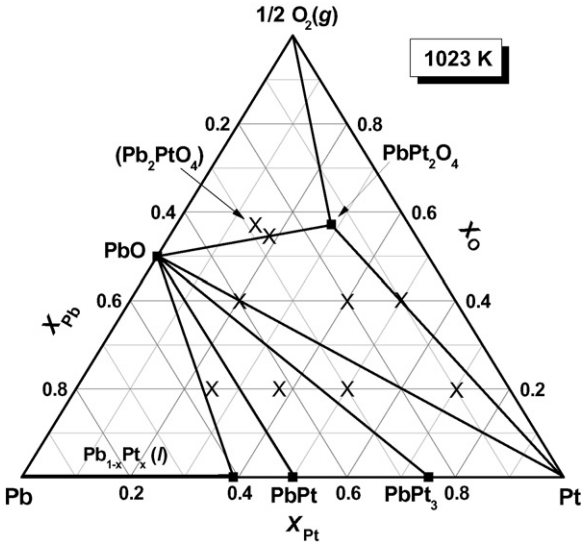


**Fig. 4.** Experimentally determined isothermal section of the phase diagram for the system Pb–Pt–O. The symbol × identifies the average composition of equilibrated samples.

### 3.3. Phase diagram for the system Pb–Pt–O at 1023 K

The average composition of the samples equilibrated at 1023 K, the elements and compounds used in preparing the samples, duration of equilibration, phases identified in quenched samples at room temperature and the techniques used for identification are presented in Table 1. The isothermal section of the phase diagram composed from the results obtained in this study is shown in Fig. 4. Only one ternary compound $PbPt_2O_4$ was identified at 1023 K. The compound $Pb_2PtO_4$, which was a constituent of some of the samples before equilibration, appears to have disappeared during the long equilibration. A three-phase field involving the solid phases $PbPt_2O_4$, PbO and Pt was identified.

Along the binary Pb–Pt, two intermetallic compounds $PbPt_3$ and PbPt and a liquid phase ($0 \geq X_{Pt} \geq 0.39$) were identified, in reasonable agreement with the binary phase diagram for the system [19]. All the alloy and intermetallic phases were found to coexist with PbO.

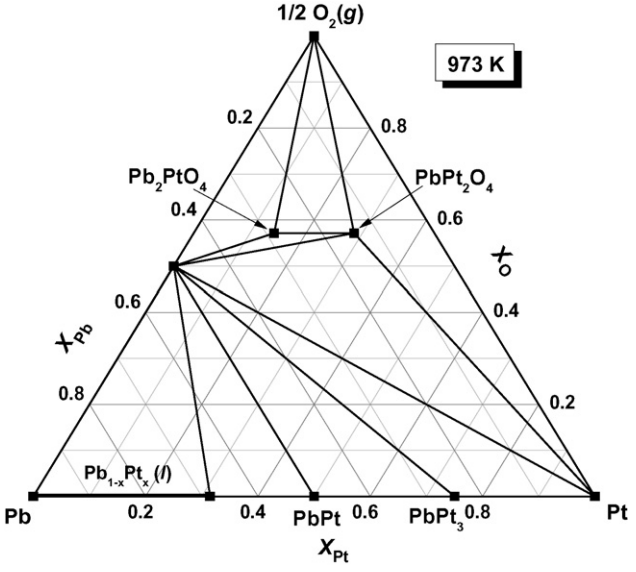


**Fig. 5.** Isothermal section of the phase diagram for the system Pb–Pt–O at 973 K calculated from thermodynamic data obtained in this study.

Based on the thermodynamic data obtained in this study, phase relations at 973 K were computed by invoking the Gibbs energy minimization principle. The result is shown in Fig. 5. At this temperature, two ternary oxides are present and an additional three-phase field involving $Pb_2PtO_4$, $PbPt_2O_4$ and PbO appears on the diagram.

## 4. Summary and conclusions

Thermodynamic properties of two lead platinum oxides were determined using solid-state cells at high temperatures. The formation reactions and the corresponding Gibbs free energies are:

$$PbO(ortho) + 2Pt + 1.5O_2 \rightarrow PbPt_2O_4$$

$$\Delta G^\circ(\pm 385)/\mathrm{J\,mol^{-1}} = -276,951 + 249.94T$$

$$2PbO(ortho) + Pt + O_2 \rightarrow Pb_2PtO_4$$

$$\Delta G^\circ(\pm 210)/\mathrm{J\,mol^{-1}} = -184,194 + 170.12T$$

Products formed by the decomposition of $PbPt_2O_4$ are equilibrium phases, whereas $Pb_2PtO_4$ yields metastable products. Equilibrium phase relations in the system Pb–Pt–O were determined by isothermal equilibration at 1023 K for extended periods.

Using estimated heat capacities, the standard enthalpies of formation from elements and standard entropies of the two ternary oxides at 298.15 K are derived. For $PbPt_2O_4$, $\Delta H_f^\circ(298.15) = -508.2(\pm 3.6)$ kJ/mol and $S^\circ_{298.15} = 186.75(\pm 3.4)$ J/mol K, and for $Pb_2PtO_4$ $\Delta H_f^\circ(298.15) = -829.1(\pm 3)$ kJ/mol and $S^\circ_{298.15} = 198.7(\pm 2.8)$ J/mol K.

## Acknowledgements

K.T. Jacob wishes to thank the Indian National Academy of Engineering, New Delhi, for support as INAE Distinguished Professor. G. Rajitha wishes to thank the University Grants Commission of India for the award of Dr. D.S. Kothari Postdoctoral Fellowship which facilitated this research.

## References

[1] P.S. Anderson, S. Guerin, B.E. Hayden, Y. Han, M. Pasha, K.R. Whittle, I.M. Reaney, J. Mater. Res. 24 (2009) 164–172.
[2] A.W. Sleight, Mater. Res. Bull. 6 (1971) 775–780.
[3] N. Bettahar, P. Conflant, F. Abraham, D. Thomas, J. Solid State Chem. 67 (1987) 85–90.
[4] S. Obbade, N. Tancret, F. Abraham, E. Suard, J. Solid State Chem. 166 (2002) 58–66.
[5] N. Tancret, S. Obbade, N. Bettahar, F. Abraham, J. Solid State Chem. 124 (1996) 309–318.
[6] K.T. Jacob, W.W. Shim, J. Am. Ceram. Soc. 64 (1981) 573–578.
[7] W.W. Shim, K.T. Jacob, Can. Metall. Quart. 21 (1982) 171–177.
[8] W.W. Shim, K.T. Jacob, J. Electrochem. Soc. 129 (1982) 1116–1121, 2385.
[9] K.T. Jacob, V.S. Saji, Y. Waseda, J. Mater. Res. 22 (2007) 1174–1181.
[10] K.T. Jacob, L. Rannesh, Mater. Sci. Eng. B 140 (2007) 53–58.
[11] K.T. Jacob, R. Subramanian, J. Mater. Sci. 42 (2007) 2521–2523.
[12] K.T. Jacob, R. Subramanian, J. Phase Equilib. Diffus. 29 (2008) 136–140.
[13] K.T. Jacob, G. Rajitha, V.S. Saji, Bull. Mater. Sci., submitted for publication.
[14] KT. Jacob, T. Uda, T. Okabe, Y. Waseda, J. Chem. Thermodyn. 32 (2000) 1399–1408.
[15] G. Periaswami, S.V. Varamban, S.R. Babu, C.K. Mathews, Solid State Ionics 26 (1988) 311–317.
[16] O. Kubaschewski, C.B. Alcock, Metallurgical Thermochemistry, 5th ed., Pergamon Press, New York, 1979.
[17] M.W. Chase Jr., NIST-JANAF Thermochemical Tables, 4th ed., Part-II. Monogragh No. 9, Journal of Physical and Chemical Reference Data, American Institute of Physics, New York, 1998, pp. 1722–1745.
[18] L.B. Pankratz, Thermodynamic Properties of Elements and Oxides, Bulletin 672, United States Department of the Interior, Bureau of Mines, Washington, D.C., 1982, pp. 93–475.
[19] T.B. Massalski, P.R. Subramanian, H. Okamoto, L. Kacprzak (Eds.), Binary Alloy Phase Diagrams, vol. 3, 2nd ed., ASM International, Materials Park, OH, 1990.